Available online at www.sciencedirect.com
SCIENCE DIRECT®
Journal of Crystal Growth 252 (2003) 58–67
JOURNAL OF CRYSTAL GROWTH
www.elsevier.com/locate/jcrysgro

Effect of dissimilar anion annealing on structures of InAs/GaAs quantum dots

Y.Q. Wang[a], Z.L. Wang[a], J.J. Shen[b], A. Brown[b,*]

[a] School of Materials Science and Engineering, Georgia Institute of Technology, Atlanta, GA 30332, USA
[b] School of Electrical and Computer Engineering, Georgia Institute of Technology, Atlanta, GA 30332, USA

Received 26 July 2002; accepted 10 December 2002
Communicated by A.Y. Cho

Abstract

In this paper, we report microstructural characterization of InAs/GaAs quantum dots grown by molecular beam epitaxy. The InAs islands were annealed in a range of temperatures under Pa flux. Prior to annealing, it is shown that the InAs islands are mainly lens-shaped, mostly vertically self-aligned and coherent to GaAs (100) substrate. Relaxation by misfit dislocations is occasionally found. Abnormal relaxation is observed in larger islands. Stacking faults in a V-shape are frequently formed in the lateral sides of these regions. No obvious change in island density and self-alignment occurred when the dots are annealed under Pa flux at 300°C. In contrast, remarkable changes took place upon annealing at 350°C. The vertically self-aligned islands disappear, and smooth interfaces were obtained. This morphological transition is argued to result from the replacement of arsenic by phosphorus in the InAs dots. The damage to the crystalinity of the abnormally relaxed regions cannot be removed by the post-growth annealing. The remarkable morphological transition by post-growth annealing under dissimilar anion atmosphere offers another possibility for tuning the dot morphology and hence their electronic properties.

Keywords: A1. Anion exchange; A1. Vertical self-alignment; A3. Molecular beam epitaxy; A3. Quantum dots; B1. InAs

1. Introduction

The III–V compound semiconductor quantum dots (QDs), grown by molecular beam heteroepitaxy (MBE) in the Stanski–Krastanov (S–K) growth mode, are important for many novel electronic properties and device applications [1,2]. The great potential of QDs as active medium for devices was recognized in early 1980s [3,4]. Leonard [5] in 1993 showed the feasibility of self-organized QDs by heteroepitaxy, and then Ledentsov et al. [6] and Xie et al. [7] demonstrated lasing of self-organized and vertically self-organized InAs QDs, respectively. Since then, extensive works have been done and great progress has been made in both theory and device applications, as reviewed, for example, in Ref. [8].

The unique electronic properties of QDs originate from their 5-function like density of states and ultimate confinement of electron and hole wave functions. They strongly depend upon not only the chemistry and strain status, but also the

*Corresponding author. Tel.: 404-894-8008; fax: 404-894-9140.
E-mail address: abrown@ee.duke.edu (A. Brown).

0022-0248/03/$ - see front matter
doi:10.1016/S0022-0248(02)02527-7

size, size uniformity and shape of the QDs [10]. Any accurate interpretation of the measured electronic properties is only possible when all of the information about QDs is available. Presently, several experimental techniques, such as transmission electron microscopy (TEM) [11,12], grazing incidence X-ray diffraction [13], top-view atomic force microscopy (AFM) or scanning-tunneling microscopy (STM) [14,16], have been employed to characterize the dot morphologies.

For most of device applications, vertically stacked QDs are desirable. It has been shown that the dot size distribution and a vertical alignment need to be optimized among the growth conditions, including spacer thickness [17], material coverage [18], growth interruption [19], the number of periods of the multilayer [20,21], growth rate [22], post-growth annealing [23], and substrate miscut angle [24]. The physics behind them is the mechanical or elastic interaction of the islands via their strain fields. When the islands nucleate from a plain substrate (strain free and defect-free), the nucleation and growth are completely homogeneous and random processes. In contrast, the nucleation and growth become quite inhomogeneous when there is an island layer embedded beneath the substrate surface. The strain field associated with the embedded islands first affects the nucleation process in such a way that the islands in the subsequent layer nucleate preferentially right above the embedded islands. The strain fields of the embedded islands will further enhance the growth of these newly born islands. This preferential localization of the island formation gives rise to the improved size uniformity and vertical alignment.

We have been investigating the modification of quantum dot size, composition, strain, and optical properties via changes in growth conditions and the use of dissimilar anion anneal steps after formation of the dots. In our anion exchange approach, the InAs quantum dots are annealed under a P_2 flux. Previous works [9,15,25] have shown that (1) P-for-As anion exchange, or intermixing of P and As in the top surface InAs layer, occurs during P_2 anneal; (2) the P_2 anneal of InAs quantum dots can change the quantum dot morphology remarkably depending on the annealing temperature. In this work, we will focus on TEM stuctural characterization of the InAs/GaAs multi-layered QD structures with/without dissimilar anion annealing. We will demonstrate that anion exchange is an effective approach to modify vertical alignment and island size uniformity in MBE-grown InAs/GaAs dot superlattice structures.

2. Experimental procedure

The epitaxial films were grown by molecular beam epitaxy on semi-conducting (0 0 1)-GaAs substrates using As_4 and P_2 produced by a solid valued cracker source. After growing a 100 nm GaAs buffer layer at the deoxidization temperature of 580°C, three nominal monolayers (MLs) of InAs were deposited at 450°C. There are five layers of 3-ML InAs, which are separated by 10 nm GaAs spacers. The top InAs layer is left uncapped. A V/III (As_4/In) flux ratio of 18 was used in the growth of InAs. The growth rate was about 0.25 ML/s. After the growth of each InAs layer, the samples were ramped down to a temperature below 450°C and annealed at these temperatures for 3 min. During the annealing, the surface was fluxed by P_2 with a beam equivalent pressure of 2.7×10^{-6} Torr. The exposure of the surface to an atmosphere of a dissimilar anion is a unique approach for this experiment. We expect that the dot morphologies can be controlled and tailored by a possible anion exchange at the surface.

Reflection high-energy electron diffraction (RHEED) was used to monitor the surface morphology transitions during the growth and the annealing. A spotty pattern signaled the formation of the three-dimensional islands or QDs. It was observed that the spotty pattern was unchanged during As4 fluxing. However, during P_2 annealing, the RHEED pattern can change considerably depending on the annealing temperature. The structural characterization and EDX analysis have been conducted in a JEOL 4000EX HRTEM operated at 400 kV and Hitachi HF-2000 STEM (scanning transmission electron microscope) operated at 200 kV. The [1 1 0]/[1 $\bar{1}$ 0]

cross-sectional TEM specimens were prepared by gluing two growth surfaces together with M-610 crystal bond. The specimens were bonded in such a way that one-half was along the [1 1 0] orientation and the other along the [1 $\bar{1}$ 0] orientation so that the heterostructure could be examined simultaneously along both directions. The glue should be thick enough to prevent interference from the other half during comprehensive tilting TEM analysis.

3. Results and discussion

Fig. 1 shows typical (0 0 4) bright field images (BFIs) and dark field images (DFIs) of the multi-layered quantum dot structure with no anneal. The InAs islands or dots are revealed, mainly by the strain contrast, to be well defined and with a half-lens shape. The vertical alignment of the InAs dots can be seen more clearly in the enlarged BFI (Fig. 1c) and DPI (Fig. 1d). As will be shown by high-resolution TEM (HRTEM), most of the well-defined dots are coherent to the GaAs spacers. Although the islands appear, under the TEM, to take the half lens-shape with a height of about 3 nm, and a lateral size of about 15 nm, as indicated by the dotted lines in Fig. 1c, the actual shape of the islands still remains to be an issue for open discussion.

It should be noted that the strain field of the aligned islands is well extended into the substrate, which implies that neglecting of this part of strain energy may lead to considerable deviation in predicting the critical conditions, e.g., critical thickness, for the morphology transition.

The enlarged images Fig. 1(e) and (f) show the abnormally relaxed morphologies of the vertically aligned dots. The reason why we say "abnormally" rather than "plastically" will become apparent later. The abnormally relaxed regions are usually bounded by V-shaped stacking faults, which are formed from the two lateral sides of these regions, much larger than the coherent islands, but rather poor defined.

The islands and abnormally relaxed regions can appear quite different depending on the imaging conditions. Fig. 2 is a representative example of

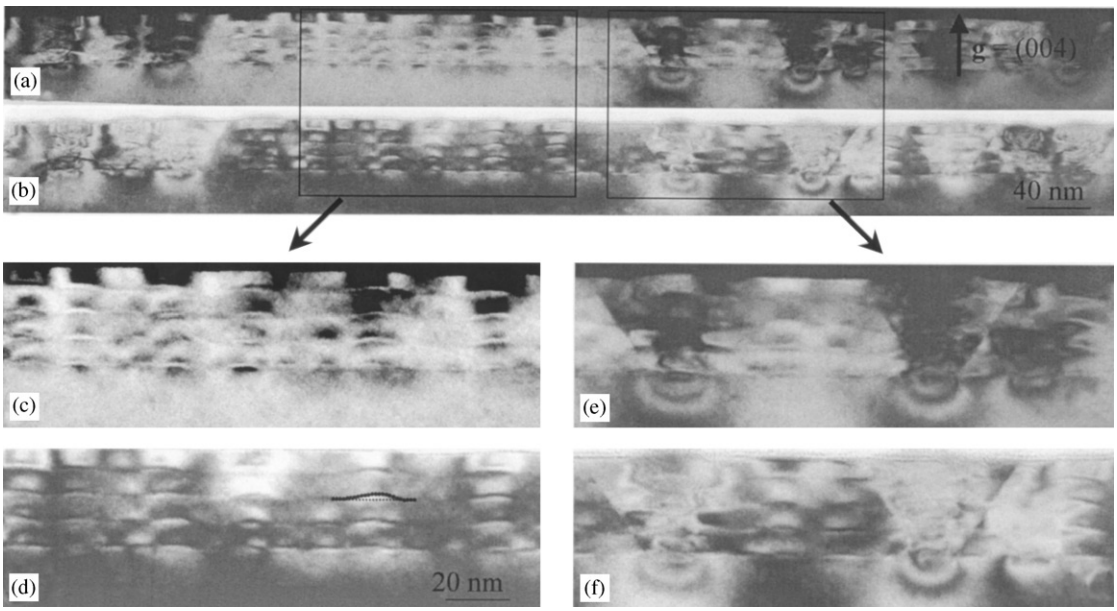

Fig. 1. TEM images ((0 0 4) dark-field images (a) and corresponding bright-field images (b)) showing the multi-layered quantum dots. The vertical alignment of the quantum dots can be seen more clearly in the enlarged bright-field images (c) and dark-field image (d). These dots are mostly coherent to the GaAs spacers. The enlarged bright-field image (e) and dark-field image (f) show the complicatedly relaxed morphologies of the vertically aligned dots.

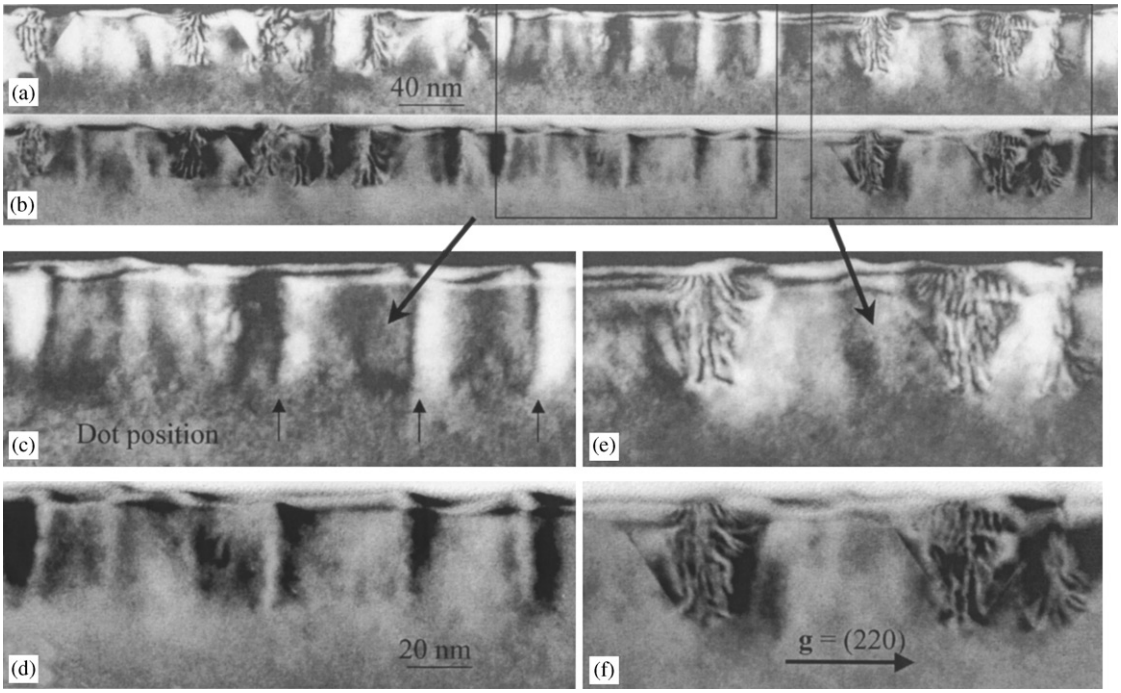

Fig. 2. The (2 2 0) dark-field images and bright-field images showing the multi-layered quantum dots. As compared to the (0 0 4) images, the vertically aligned dots and abnormally relaxed regions show different morphologies.

the same area as Fig. 1. In this case, the operative reflection is (2 2 0), normal to the growth direction. As compared with the (0 0 4) image, the islands are shown as bright bands (in BFI, Figs. 2a and c) or dark bands (in DFI,Figs. 2b and d) under the (2 2 0) imaging conditions. This is a good indication of the overlapping strain fields related to the vertical alignment of the islands. For the operative reflections inclined to the interface, e.g. (1 1 1), the islands are imaged as distorted half-lens shape. Since no further crystallographic information can be extracted from them, the reflections inclined to the interface are not suggested for dot observations.

The abnormally relaxed regions are revealed as a much more different morphology under (2 2 0) imaging conditions, as shown in Figs. 2e and f. It can be seen that the fringed patterns are also V-shaped, indicating that the island size becomes larger and larger with the increase in the number of layers. Due to the strong interaction between the dots in adjacent layers, the nature of the relaxation is difficult to identify. The dark and bright contrast modulation had initially been thought to be Moiré fringes, which is usually direct evidence that islands are plastically relaxed. If this was true, one could estimate that about half of the misfit strain (7.2%) was relaxed by using the fringe distance (about 5.0 nm for (2 2 0) imaging conditions). However, as shown later by the chemistry analysis and HRTEM, the contrast mechanism is far more complicated, and cannot be explained by plastic relaxation alone.

It should be noted that the abnormally relaxed regions hardly shows any particular features under (0 0 2) or (0 0 4) imaging conditions, except the frequent two V-shaped stacking faults. In contrast, when the image is formed using a beam inclined to the interface, the fringe pattern will be revealed. This visibility of the fringes suggests that there exists possibly some lateral compositional modulation in these regions.

Fig. 3 shows three typical indium EDX line scans taken along the growth direction. Qualitatively, the peak indicates a relative change in the In-concentration, the higher the In-concentration,

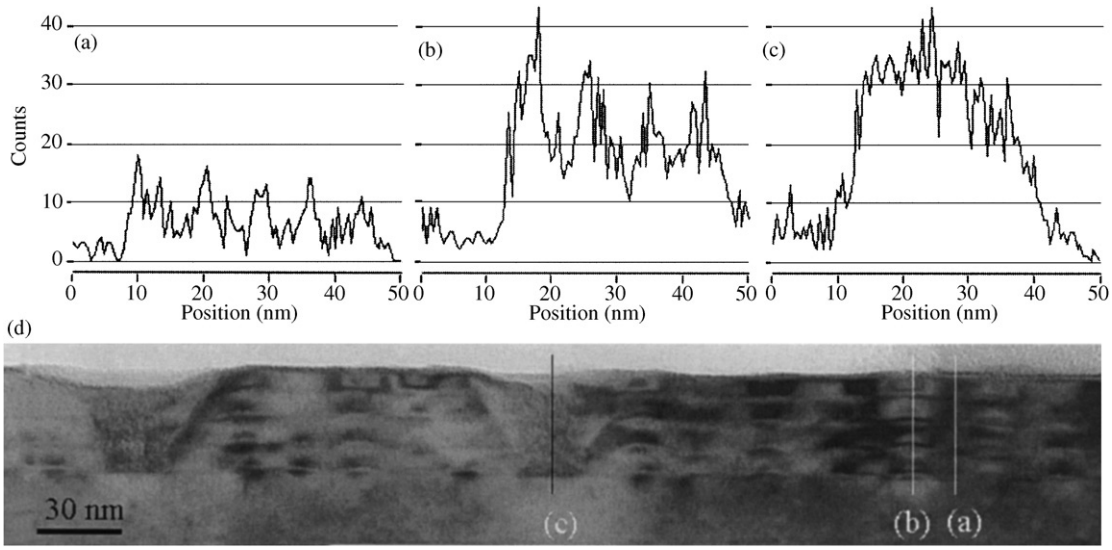

Fig. 3. EDX line scan indium profiles through (a) the wetting layers, (b) the vertically aligned dots, (c) the abnormally relaxed region. The scanning lines are indicated in the STEM image (d).

the higher the peak is. The first scan passes through the wetting layer, and the five small In-peaks correspond to the five wetting layers (Fig. 3a). The second scan passes through the apexes and central regions of the islands. As shown in Fig. 3b, much higher In-peaks appear when the electron beam scans through the islands. The EDX line scan indium concentration profiles clearly demonstrate the formation of the islands. The third scan is taken through the abnormally relaxed region. In contrast to the scans through islands or wetting layer, there is only a broad peak over this region, indicating a uniform distribution of indium. By comparing the area under the peak in the three scans, the total amount of indium is much higher in the abnormally relaxed regions. EDX quantitative analysis shows that the In concentration in these regions varies between 10% and 15% atm. These results indicate that there is a large degree of intermixing between Ga and In cations, leading to much more relaxation in these regions (the $In_xGa_{(1-x)}As$ alloy formed through intermixing causes a misfit strain of up to 2.1%, about one third of that for InAs). During the deposition of InAs, the growth is much enhanced possibly owing to the relaxation and segregation of In atoms. Since the abnormally relaxed regions are only observed in the 3 ML samples (in our 2 ML samples, we have observed no such phenomenon), their formation appears to be related with the islands with a larger size.

HRTEM observation shows that most of the well-defined InAs islands are coherent to the surrounding GaAs in spite of some elastic relaxation. However, some of them are plastically relaxed. Such an example is shown in Figs. 4a and b, where a 60° misfit dislocation is formed in the interface between the dot base and the GaAs barrier layer. The 90° misfit dislocations have also been observed, but much less frequently. Another interesting result is that dislocation dipoles are also observed in some plastically relaxed dots, as shown in Figs. 4c and d. Dislocation dipoles have been reported by Wang et al. in GaInP/GaAs heterostructures [27], who suggested that the dipole dislocations were formed due to the compositional modulation in the GaInP phase. In the dot case, the dislocation dipoles seem to have formed by a different mechanism. When the dot grows to a critical size, a misfit dislocation is formed first in the interface between the base and the lower barrier layer. The formation of this dislocation relaxes much of the coherent strain and the top part of the dot assumes a lattice constant

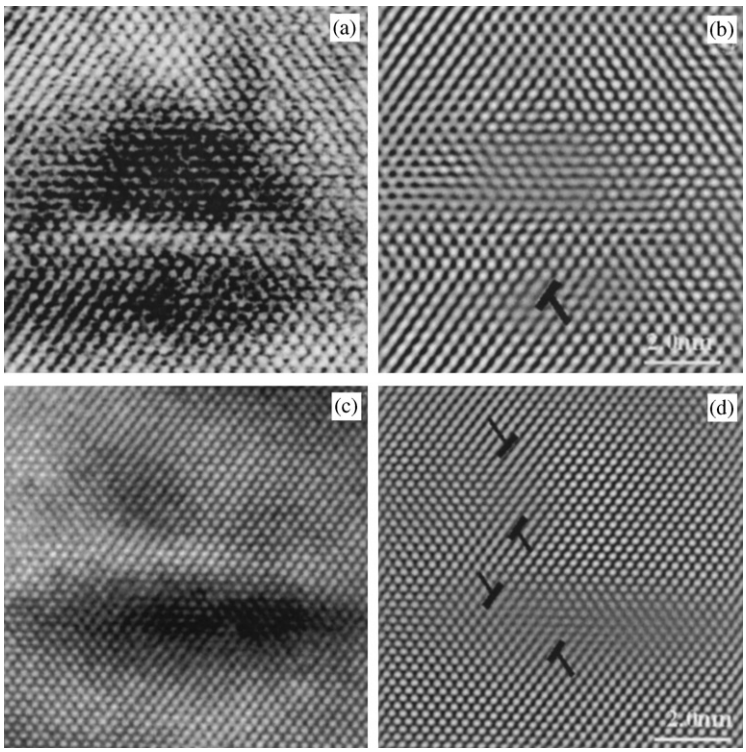

Fig. 4. HRTEM images of the relaxed dots by a 60°C dislocation (a) and a dislocation dipole (c). (b) and (d) are Fourier filtered images.

much close to that of InAs. During the growth of the upper GaAs barrier layer, the dot (mainly the top part) is compressed and the contact part in the barrier is stretched to keep coherency. If energetically favorable, another misfit dislocation may form at the interface between the dot and the upper barrier layer. Considering the energetics and the strain involved, a dislocation dipole should be the most favored configuration. So far, no work has been reported on how the misfit dislocations may affect the vertical alignment. The introduction of one 60° misfit dislocation into the QW can relax most of the strain. Since the strain field is commonly considered to play a central role in the vertical alignment of the dots, one may expect its relaxation should have considerable impact on the alignment. However, we have not observed such a phenomenon in our samples no matter in which layer the relaxed dots are located.

The HRTEM image of the abnormally relaxed regions is shown in Fig. 5. The remarkable feature in these regions is the large lattice distortion and a large number of crystal defects, including stacking faults and dislocations. However, no dislocations have found along the lateral boundary. The fringe contrast in the image is mostly related with the distortion bands. By measuring the change of the local lattice constants, it can be shown that the lattice distortion is not uniform, indicative of a non-uniform distribution of In atoms in this region. Even in the HRTEM image, the islands in each layer cannot be distinguished from the barrier layers. This further supports the argument that large-degree intermixing of In and Ga atoms has happened during the deposition.

Intermixing of cations is a well-recognized phenomenon during the deposition of the spacer layer. The region close to the island apex is mostly relaxed and the lattice constants are mostly different from those of GaAs. During the growth of the barrier layer, the materials of GaAs around the islands will try to compress the islands and

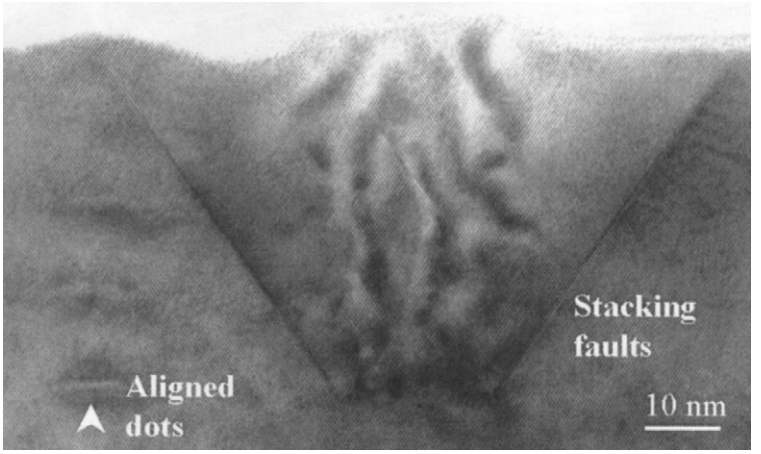

Fig. 5. HRTEM image of the abnormally relaxed morphology. The lattice is remarkably distorted and there are a large number of dislocations and stacking faults in these regions. The size of the relaxed region appears much larger than that of one column of dots.

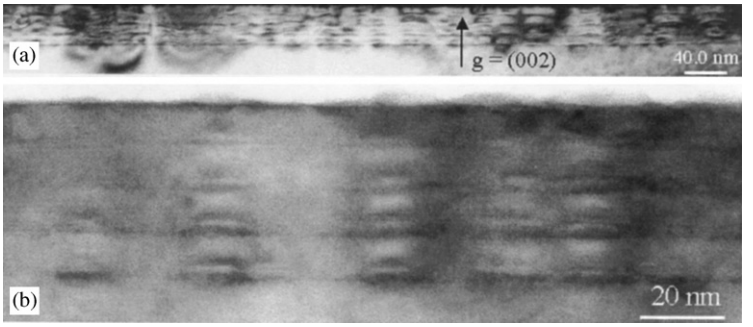

Fig. 6. The (0 0 2) dark-field image (a) and HRTEM image (b) of the multi-layered structure annealed under P_2 flux at 300°C. The vertically aligned dots and the abnormally relaxed regions show virtually no change by annealing.

therefore the materials in the islands tend to be squeezed out. This tendency of Ga-pushing-in and In-squeezing-out leads to the Ga/In intermixing and morphological change. Garcia et al. systematically studied the morphological changes of the self-assembled InAs islands at the initial stages of the GaAs overgrowth by using AFM [28]. Their results showed direct evidence that the height of the islands was reduced from the original 10.0 nm to about 3.0 nm due to the large redistribution of the materials or In/Ga intermixing. It can be imagined that the larger the islands, the more difficult is their coherent burial and hence the more intermixing, as observed in our samples. When the islands are large enough to introduce misfit dislocations and they are relaxed to their own lattice constants, the burial may not be achieved at all. Lin et al. have observed that the InAs islands formed by 5 ML deposition underwent a novel morphological transition during the deposition of GaAs [29]. The disk-shaped islands were transformed into ring-shaped ones. InAs became depleted in the central region of what had been a disk-shaped InAs island, resulting in the formation of crater-like surface depressions. Similar surface features were also observed during the burial of the 2 ML InAs islands [28].

Our experiment shows that post-growth annealing under P_2 flux at 300°C causes no obvious change in the island density, self-alignment and other morphological aspects. A typical example is shown in Fig. 6. As annealing temperature

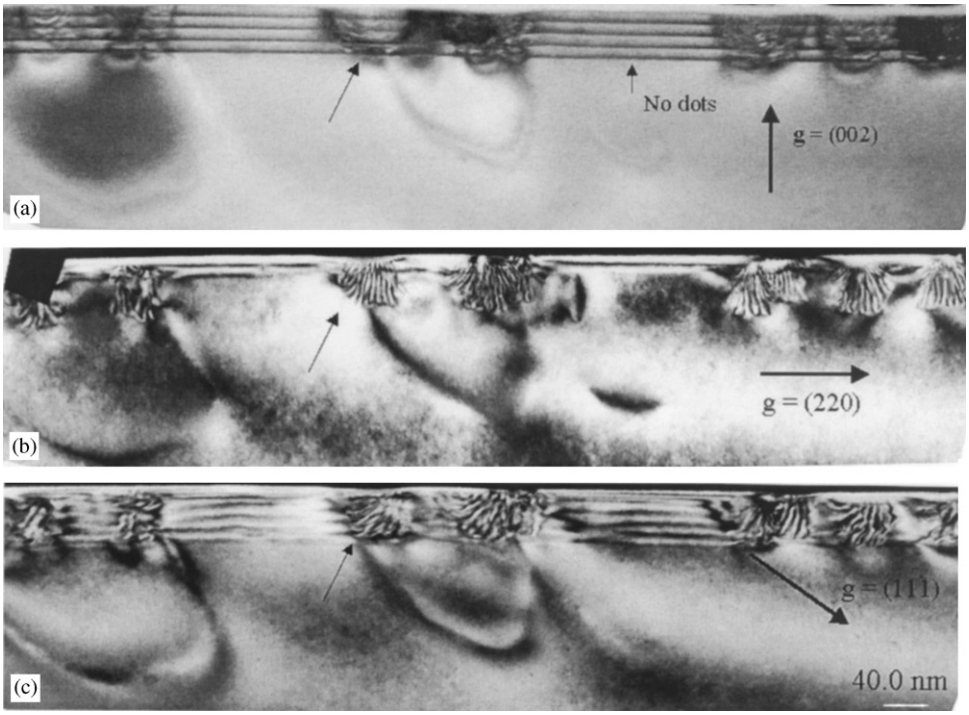

Fig. 7. Dark-field images of the InAs/GaAs multi-layered heterostructure annealed under P_2 flux at 350°C. The InAs islands have mostly been annealed out through a mechanism involving As and P exchange. Note the dislocation half-loops are formed from the bottom of the complicatedly relaxed regions, (a) The (0 0 2) dark-field image; (b) the (2 2 0) dark-field image; (c) the (1 1 1) dark-field image.

increases to above 300°C, the island morphology begins to change gradually. Remarkable changes take place upon annealing at 350°C. Fig. 7 shows the structure imaged under different conditions. Clearly, the vertically aligned islands have disappeared, and planar growth fronts and hence smooth interfaces are obtained. This observation is in agreement with the RHEED pattern, which changes gradually from spotty to streaky during annealing, and AFM observations, which directly show a flat surface morphology with a lot of fine structures [25]. Our HRTEM observation also shows the disappearance of the island structure after P_2-annealing at 350°C, as shown in Fig. 8. However, the interfaces can be seen rough and diffusing at the atomic scale.

Although the vertically aligned islands are annealed out due to anion exchange, and leave behind no trace of their previous existence. The opposite effect is observed in the abnormally relaxed regions. As shown in Fig. 7, the position of these regions was unchanged and similar fringe contrasts are still present, suggesting that the relaxed microstructure, which is caused possibly by intermixing of In and Ga, misfit dislocation, interfacial roughening, and/or other mechanisms, cannot be annealed away by the P_2 annealing. This may be understandable, considering that the possible anion exchange occurs on the interface whereas the relaxed regions are three-dimensional. In Fig. 7, we also show that half dislocation loops are generated from the bottom of the abnormally relaxed regions and extend into the GaAs substrate. Based on the contrast change in the two-beam imaging conditions, these dislocation loops have Burgers' vectors which are in the {1 1 1} planes inclined to [1 1 0].

The above-described morphological transition is argued to result from the replacement of arsenic by phosphorus in the InAs dots and the InAs wetting layers. This anion exchange has been predicted to be favorable thermodynamically under typical

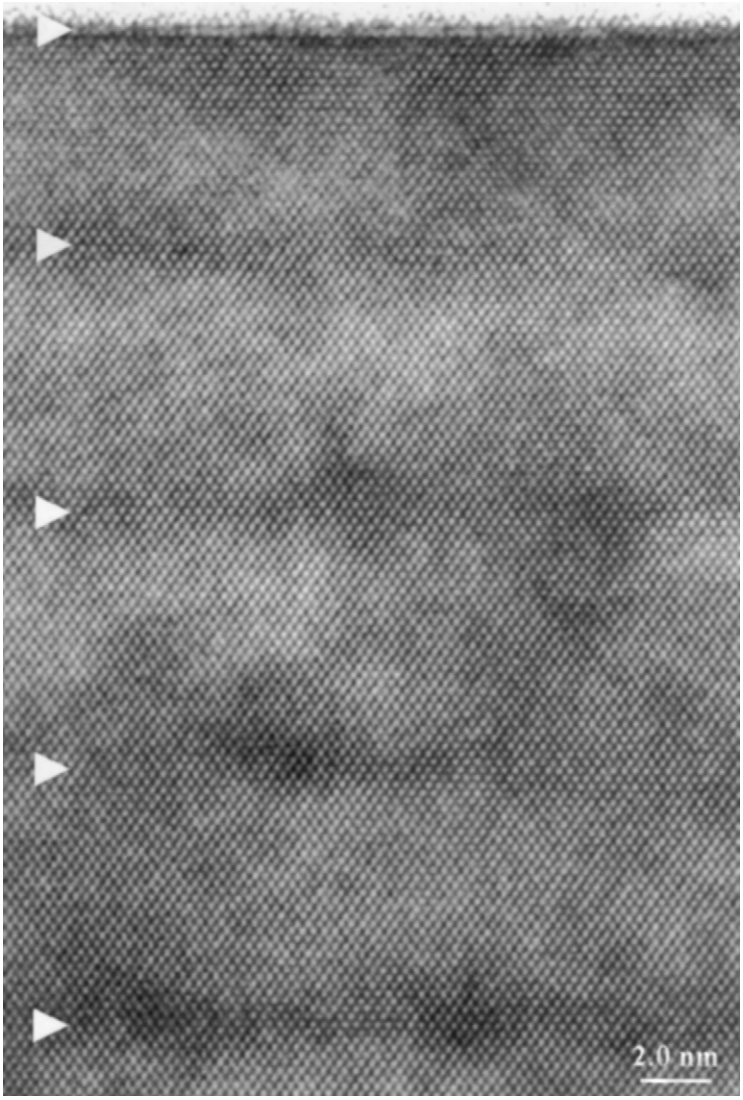

Fig. 8. HRTEM of the InAs/GaAs multi-layered structure after annealing under P_2 at 350°C. The InAs dots have been removed by annealing through the anion exchange mechanism. Note the interfaces are rough and diffuse.

epitaxial conditions [26]. As a result of the P-for-As anion exchange, a ternary $InAs_xP_{(1-x)}$ alloy layer is formed in the topmost surface of the dot layer, and the coherent strain energy, the driving force for the 2D-to-3D growth, is reduced due to the smaller lattice-mismatch. This reduction in the strain energy will decrease the stability of the islands, and enhance the mass transport from the islands to the wetting layer, leading to shrinkage of the islands. Therefore, during P_2 annealing, two opposite processes occur simultaneously. One is island coarsening via Ostwald ripening, and the other is island shrinkage due to anion exchange. A detailed discussion of these two processes and the energetics under the dissimilar anion annealing conditions has been presented elsewhere [9].

One important implication of the change in the InAs island morphology under dissimilar anion annealing conditions is that anion exchange reaction can be used to tailor the island size and

to improve size uniformity. Islands of larger or smaller sizes can be obtained simply by appropriately controlling the annealing conditions, such as annealing temperature and beam flux. Under our present conditions, the shrinkage caused by the P-for-As anion exchange apparently dominate over the Ostwald ripening, leading to the complete disappearance of islands. Since the high strain energy concentration along the island edges favors more exchange, the large islands shrink faster than smaller ones. This offers a mechanism to enhance the size uniformity and vertical alignment by the P-for-As anion exchange. Significant improvement in InAs island size uniformity and vertical alignment in a multi-layer quantum dot structure have been demonstrated [9].

4. Conclusion

The microstructure of MBE-grown InAs/GaAs quantum dots annealed under P2-flux in a temperature range below 450°C has been examined by TEM. It is concluded that the InAs islands separated by 10 nm GaAs spacer are vertically self-aligned and are mostly coherent to GaAs (1 0 0) substrate. Much more complicated relaxation is observed in larger islands. Postgrowth annealing in P_2 flux below 300°C gives rise to no obvious change in island density and self-alignment. In contrast, the vertically self-aligned islands can be removed completely by P_2-annealing at 350°C, although the damage to the crystalinity of the abnormally relaxed regions cannot be annealed away. The remarkable morphological transition by post-growth annealing under dissimilar anion atmosphere offers another possibility for tuning the dot morphology and hence the electronic properties.

References

[1] V.V. Mitin, V.A. Kochelap, M.A. Stroscio, Quantum Heterostructures: microelectronics and optoelectronics, Cambridge University Press, Cambridge, New York, 1999.
[2] D. Bimberg, Semiconductors 33 (1999) 951.
[3] A.I. Ekimov, A.A. Onushzhenko, JETP Lett. 34 (1981) 2225.
[4] Y. Arakawa, H. Sakaki, APL 40 (1982) 939.
[5] D. Leonard, M. Krishnamurthy, C.M. Reaves, S.P. Denbaars, P.M. Petroff, Appl. Phys. lett. 63 (1993) 3203.
[6] N.N. Ledentsov, V.M. Ustinov, A.Yu. Egorov, A.E. Zhukov, M.V. Maksimov, I.G. Tabatadze, P.S. Kop'ev, Semiconductors 28 (1994) 832.
[7] Q. Xie, A. Kalburge, P. Chen, A. Madhukar, IEEE Photon. Technol. Lett. 8 (1996) 965.
[8] M. Bimberg, N.N. Grundmann, Ledentsov, Quantum dot Heterostructures, Wiley, Hichester, New York, 1999.
[9] Y.Q. Wang, Z.L. Wang, J.J. Shen, A.S. Brown, Engineering vertically-aligned InAs/GaAs quantum dot structures via anion exchange, Solid State Commun. accepted for publication.
[10] M. Grundmann, O. Stier, D. Bimberg, Phys. Rev. B 59 (1999) 5688.
[11] J. Zou, X.Z. Liao, D.J.H. Cockayne, R. Leon, Phys. Rev. B 59 (1999) 12279.
[12] X.Z. Liao, J. Zou, X.F. Duan, D.J.H. Cockayne, R. Leon, C. Cobo, Phys. Rev. B 58 (1998) R4235.
[13] K. Zhang, Ch. Heyn, W. Hansen, Appl. Phys. Lett. 77 (2000) 1295.
[14] J.M. Garcia, G. Medeiros-Ribeiro, K. Schmidt, T. Ngo, J.L. Feng, A. Lorke, J. Kotthaus, P.M. Petroff, Appl. Phys. Lett. 71 (1997) 2104.
[15] J.J. Shen, A. Brown, Y.Q. Wang, Z.L. Wang, J. Vac. Sci. Technol. B 19 (4) (2001) 1463.
[16] O. Flebbe, H. Eisele, T. Kalka, F. Heinrichsdorff, A. Krost, D. Bimberg, J. Vac. Sci. Technol. B 17 (1999) 1639.
[17] Q. Xie, A. Madhukar, P. Ch, N.P. Kobayashi, Phys. Rev. Lett. 75 (1995) 2242.
[18] E. Scholl, S. Bose, Solid State Electron. 42 (1998) 1587.
[19] Y.W. Zhang, S.J. Xu, C.H. Chiu, Appl. Phys. Lett. 74 (1999) 1809.
[20] J. Tersoff, Phys. Rev. Lett. 76 (1996) 1675.
[21] Y. Furukawa, S. Soda, M. Ishii, A. Wakahara, A. Sasaki, J. Electron. Mater. 28 (1999) 452.
[22] M.A. Al-khafaji, A.G. Cullis, M. Hopkinson, D.J. Nowbray, M.S. Skolnick, Inst. Phys. Conf. Ser. 164 (1999) 111.
[23] J.P. McCaffrey, M.D. Robertson, Z.W. Wasilewski, S. Fafrard, L.D. Madsen, Inst. Phys. Conf. Ser. 164 (1999) 107.
[24] R. Leon, C. Lobo, A. Clark, R. Bozek, A. Wysmolek, A. Kurpiewski, M. Kaminska, J. Appl. Phys. 84 (1998) 248.
[25] J.J. Shen, A.S. Brown, R.A. Metzger, B. Sievers, L. Bottomley, P. Eckert, W.B. Carter, J. Vac. Sci. Technol. B 16 (1998) 1326.
[26] Y.Q. Wang, Z.L. Wang, T. Brown, A. Brown, G. May, Thermodynamic analysis of anion exchange during heteroepitaxy, J. Crystal Growth 242 (2002) 5.
[27] Y.Q. Wang, Z.L. Wang, T. Brown, A. Brown, G. May, Appl. Phys. Lett. 77 (2000) 223.
[28] J.M. Garcia, G. Medeiros-Ribeiro, K. Schimidt, T. Ngo, J.L. Feng, A. Lorke, J. Kotthaus, P.M. Petroff, Appl. Phys. Lett. 71 (1997) 2015.
[29] X.W. Lin, J. Washburn, Z. Liliental-Weber, E.R. Weber, A. Sasaki, A. Wakahara, Y. Nabetani, Appl. Phys. Lett. 65 (1994) 1677.